

Towards Integrated Optical Quantum Networks in Diamond

Andrei Faraon^{*}, Charles M. Santori, Zhihong Huang, Victor M. Acosta, Paul E. Barclay,
Kai-Mei C. Fu, Raymond G. Beausoleil

Hewlett Packard Laboratories, 1501 Page Mill Rd., Palo Alto, CA, 94304, USA

ABSTRACT

We demonstrate coupling between the zero phonon line (ZPL) of nitrogen-vacancy centers in diamond and the modes of optical micro-resonators fabricated in single crystal diamond membranes sitting on a silicon dioxide substrate. A more than ten-fold enhancement of the ZPL is estimated by measuring the modification of the spontaneous emission lifetime. The cavity-coupled ZPL emission was further coupled into on-chip waveguides thus demonstrating the potential to build optical quantum networks in this diamond on insulator platform.

Keywords: quantum information, diamond, nitrogen-vacancy center, optical resonator

1. INTRODUCTION

Nitrogen-vacancy (NV) centres in diamond are outstanding optical quantum emitters with long spin coherence times that make them one of the best candidates for solid state qubits.^{1–5} For quantum information applications, it is necessary to connect together multiple qubits,^{6,7} a task that so far has been proven difficult. Combining photonic networks with measurement-based schemes is an attractive approach for enabling scalable systems. However, many technical questions remain such as how to fabricate useful optical structures in diamond, and how to control the spectral inhomogeneity and instability of the NV center's optical transitions.^{7,8} An essential component of a quantum photonic network based on NV centers is a microcavity for enhancing the emission rate of photons into the zero-phonon line (ZPL).⁹ Here we present an approach, based on fabricating all-diamond microring and photonic crystal resonators starting from thin single crystal diamond membranes commercially available from Element 6. These structures are made by electron-beam lithography and reactive-ion etching, and are coupled to NV centers incorporated during diamond growth. For single NV centers on resonance with a cavity mode at low temperature, we have observed a spontaneous-emission lifetime reduction corresponding to more than ten-fold enhancement of emission into the zero-phonon line. The ZPL emission in the cavities was coupled into on-chip waveguides thus demonstrating the potential of these structures to build integrated optical quantum networks.

2. FABRICATION

The devices are fabricated in a diamond membrane thinned down to ~ 300 nm from a $\sim 5\mu\text{m}$ single crystal diamond membrane purchased from Element Six. For convenience, the membrane is broken into multiple shards with dimensions of few hundred microns that are placed on silicon dioxide or silicon substrates for fabrication. The first step of the fabrication is the thinning of the membrane that is done using reactive ion etching. We used oxygen plasma as the main etching recipe, but we discovered that many pits and pillars formed on the membrane when only oxygen plasma was used. The density of pits and pillars was reduced dramatically by alternating the oxygen plasma with chlorine/argon or chlorine/boron trichloride plasma.

Fig. 1 shows the sequence of the fabrication steps for the case when the membrane was placed on $2\mu\text{m}$ thick silicon dioxide substrate thermally grown on a silicon wafer. This type of substrate is appropriate for fabrication of ring resonators or ridge waveguides because silicon dioxide has a lower refractive index than diamond. After the membrane thinning, a layer of silicon nitride is deposited on the diamond. Electron beam resist is then spun on the silicon nitride, followed by e-beam writing. The pattern is first transferred in the silicon nitride using dry etching and then it is transferred in the diamond (using the silicon nitride as a mask) using dry etching in

^{*} To whom correspondence should be addressed. Email: andrei.faraon@hp.com

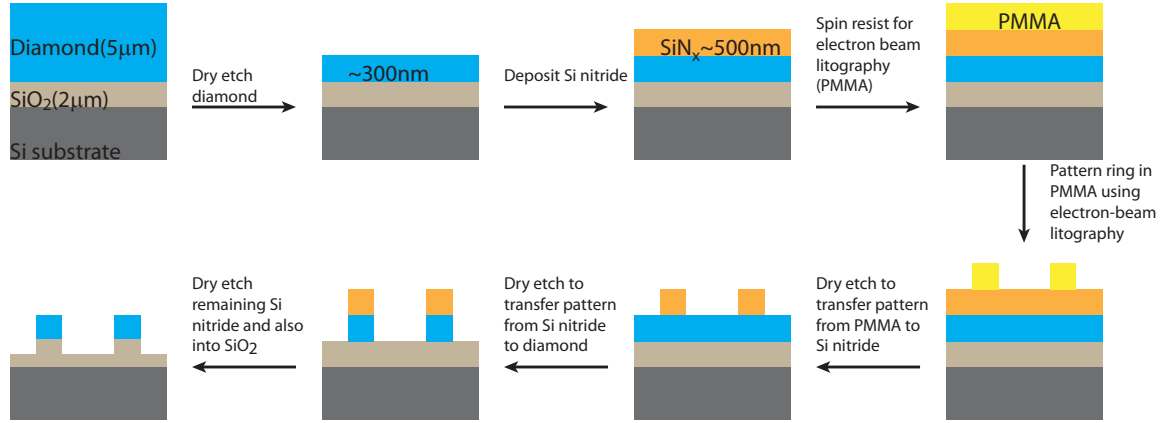


Figure 1. Schematic of the fabrication process when the diamond membrane is placed on a silicon dioxide substrate

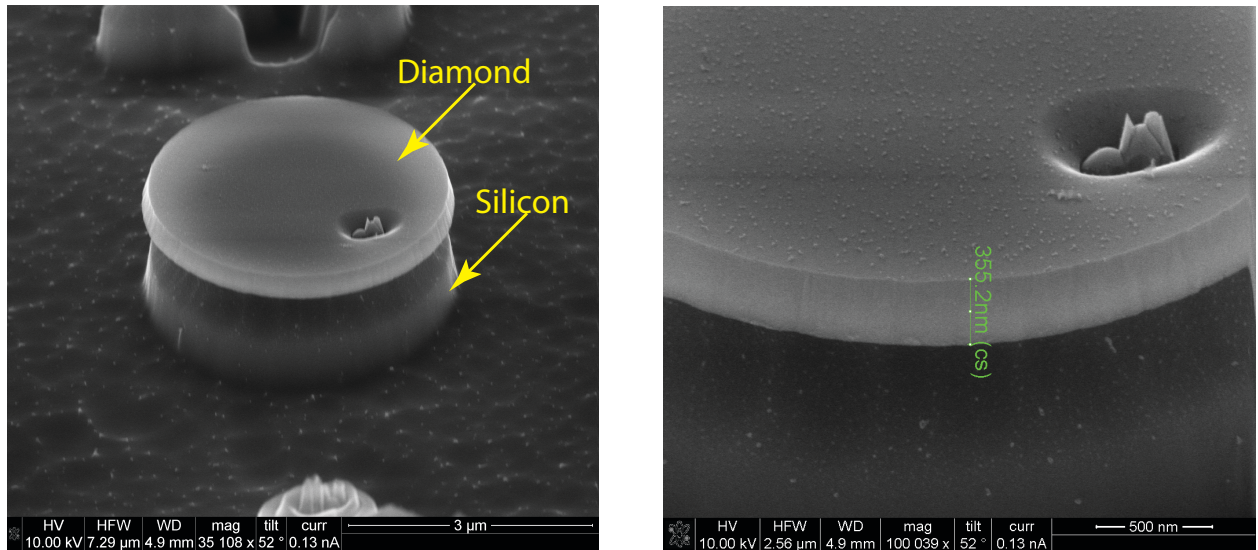


Figure 2. Diamond disk sitting on a silicon substrate. Isotropic silicon etching is used to partially etch the silicon under the diamond disk

oxygen plasma. As a variation of this process, negative resist such as HSQ can be spun directly on the diamond membrane followed by e-beam writing and etching using the resist as a mask. For some devices that needed to be suspended (as it is the case for photonic crystal devices or microdisk resonators in air) we placed the diamond membrane on a silicon substrate and used a Si isotropic etching step to partially etch the Si under the diamond membrane. A diamond disk fabricated using this procedure is shown in Fig. 2.

3. DEVICE CHARACTERIZATION

The microring cavities are used to enhance the photoluminescence emitted by the NV center into the ZPL. The spontaneous emission rate enhancement of a particular dipole transition i of an emitter coupled to a microresonator relative to the uniform dielectric medium of the resonator is enhanced by the factor $\left(\frac{\tau_0}{\tau_{\text{leak}}}\right)_i + F_i$,¹⁰ where $1/\tau_0$ is the emission rate in the uniform dielectric medium, $1/\tau_{\text{leak}}$ is the emission rate outside the cavity mode,

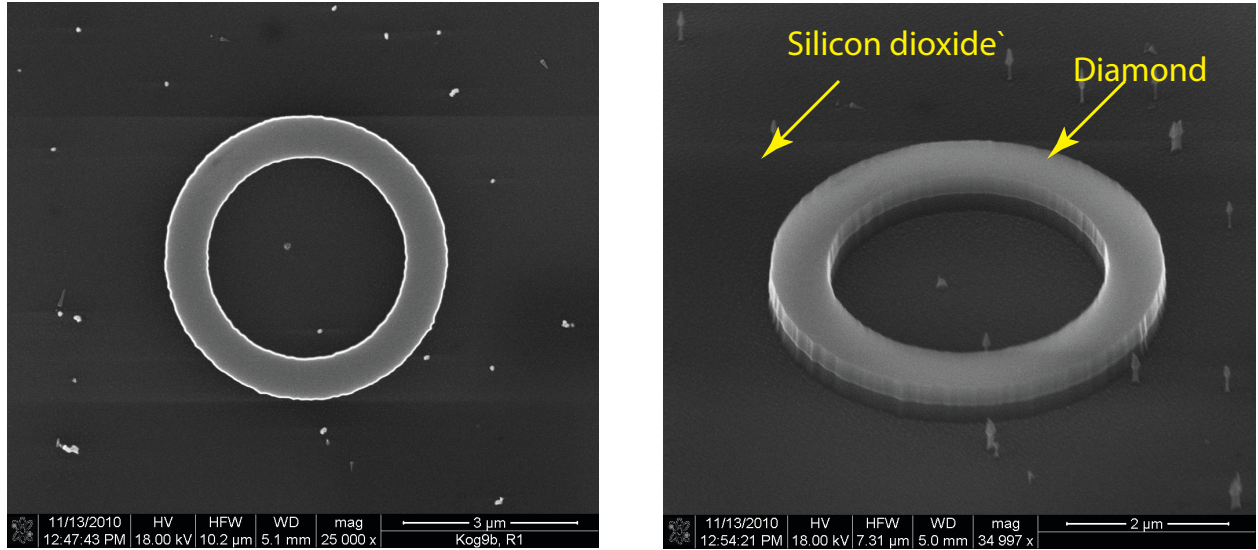


Figure 3. Diamond ring on a silicon dioxide substrate.

and

$$F_i = F_{\text{cav}} \left| \frac{\vec{E}(\vec{r}_i) \cdot \vec{\mu}_i}{|\vec{E}_{\text{max}}| |\vec{\mu}_i|} \right|^2 \frac{1}{1 + 4Q^2 \left(\frac{\lambda_i}{\lambda_{\text{cav}}} - 1 \right)^2}, \quad (1)$$

where $\vec{\mu}_i$ is the dipole moment, $\vec{E}(\vec{r}_i)$ is the local electric field at the emitter location \vec{r}_i , λ_{cav} is the cavity wavelength, λ_i is the emitter wavelength, and $|\vec{E}_{\text{max}}|$ is the maximum value of the electric field in the resonator. For the case where the dipole is resonant with the cavity and also ideally positioned and oriented with respect to the local electric field, $F_i = F_{\text{cav}}$ where,

$$F_{\text{cav}} = \frac{3}{4\pi^2} \left(\frac{\lambda_{\text{cav}}}{n} \right)^3 \frac{Q}{V_{\text{mode}}}, \quad (2)$$

n is the refractive index and $V_{\text{mode}} = \left(\int_V \epsilon(\vec{r}) |\vec{E}(\vec{r})|^2 d^3\vec{r} \right) / \max \left(\epsilon(\vec{r}) |\vec{E}(\vec{r})|^2 \right)$ is the optical mode volume of the resonator, with $\epsilon(\vec{r})$ the electric permittivity at position \vec{r} .

Eq.2 implies that the highest enhancement is obtained for cavities that have a high quality factor and a small mode volume. Microring resonators are not the first choice when small mode volume is required. However, they are relatively straight forward to fabricate and this is why we chose this type of cavity to demonstrate coupling of NV centers to microresonators.⁹ In Ref.⁹ we showed that the zero phonon line of a single NV center can be enhanced by more than a factor of ten when the cavity mode of the microring shown in Fig. 3 was tuned on resonance with the ZPL.

One advantage of using microring resonators is that they can easily be integrated in an on-chip optical network of ridge waveguides. The first step towards this integration is demonstrating the coupling between a ring and a waveguide. Towards this goal we built devices consisting of a ring resonator evanescently coupled to a ridge waveguide that is terminated with two grating couplers, as shown in Fig.4(a). The device is fabricated in single crystal diamond on a silicon dioxide substrate. To demonstrate coupling between the ring and the waveguide we performed a transmission measurement where a continuous wave tunable laser was coupled in one of the gratings and intensity of light scattered by the other grating was monitored. The transmission function is shown

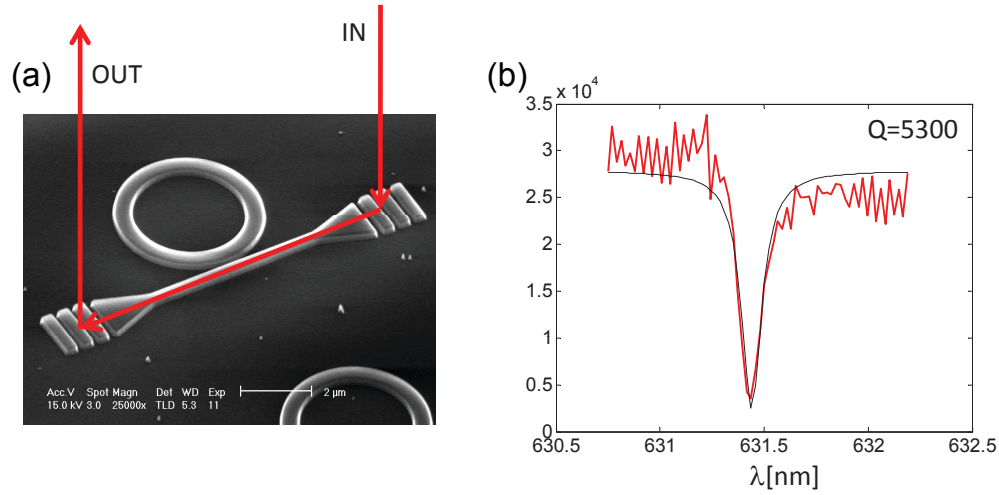


Figure 4. (a) Scanning electron microscope image of a diamond ring coupled to a ridge waveguide terminated with two grating couplers. (b) Transmission measurement of one of the ring resonances.

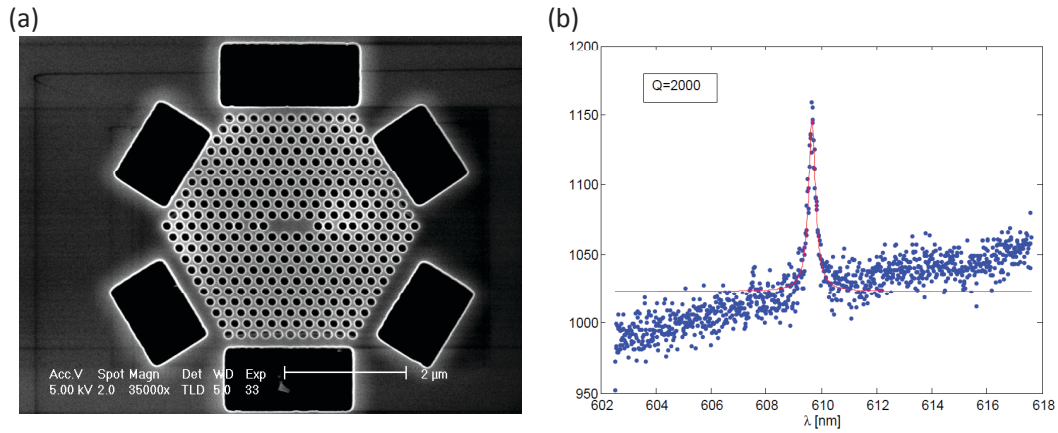


Figure 5. (a) Scanning electron microscope image of a photonic crystal cavity fabricated in single crystal diamond. (b) Photoluminescence measurement of the cavity resonance indicating a quality factor $Q \sim 2000$.

in Fig.4(b) indicating a loaded quality factor $Q \sim 5300$. A similar type of device was used to show that the photoluminescence from a NV center can be enhanced by the ring and then coupled into the waveguide.

Another type of optical resonator that can be used to enhance the ZPL is the photonic crystal cavity. Compared to microring resonators, photonic crystal cavities can have smaller mode volumes, down to one cubic wavelength, and thus can provide higher enhancement rates when the quality factor is similar. There are several designs already published in the literature.^{11,12} where the quality factor for photonic crystal cavities fabricated in single crystal diamond can reach 10^6 . We followed the design parameters reported in Ref. 11 and fabricated photonic crystal devices in the same type of material as for the microring resonators. The fabrication recipe is

the same as for undercut microdisk resonators on silicon substrate. An image of a fabricated device is shown in Fig. 5. The device was characterized using a photoluminescence (PL) measurement, where a green (532nm) laser was used to excite PL in the NV centers that was sent to a spectrometer. The fundamental mode of the photonic crystal cavity can be seen in Fig.5(b). The quality factor of this mode is $Q \sim 2000$, a factor of three lower than the quality factor expected from simulations. The discrepancy is caused by imperfections in the fabrication process. The future effort on this type of devices is to adjust the fabrication parameters such that the cavity resonance overlaps with the ZPL at 637 nm. The cavity can also be interconnected in an on-chip photonic network using photonic crystal waveguides.^{13, 14}

4. CONCLUSION

In conclusion we demonstrated micro-scale optical resonators (microrings and photonic crystal cavities) fabricated directly in single crystal diamond. These cavities were used to enhance the emission rate of nitrogen vacancy centers into the zero phonon line. The first steps have been taken towards integrating the cavities in optical networks as needed for quantum information devices for quantum chemistry¹⁵ and factoring.⁶

REFERENCES

1. F. Jelezko, T. Gaebel, I. Popa, M. Domhan, A. Gruber, and J. Wrachtrup. Observation of Coherent Oscillation of a Single Nuclear Spin and Realization of a Two-Qubit Conditional Quantum Gate. *Phys. Rev. Lett.*, 93:130501, 2004.
2. Gopalakrishnan Balasubramanian, Philipp Neumann, Daniel Twitchen, Matthew Markham, Roman Kolesov, Norikazu Mizuochi, Junichi Isoya, Jocelyn Achard, Johannes Beck, Julia Tissler, Vincent Jacques, Philip R. Hemmer, Fedor Jelezko, and Jorg Wrachtrup. Ultralong spin coherence time in isotopically engineered diamond. *Nature Mater.*, 8(5):383–387, May 2009.
3. Charles Santori, Philippe Tamarat, Philipp Neumann, Jorg Wrachtrup, David Fattal, Raymond G. Beausoleil, James Rabeau, Paolo Olivero, Andrew D. Greentree, Steven Prawer, Fedor Jelezko, and Philip Hemmer. Coherent Population Trapping of Single Spins in Diamond under Optical Excitation. *Phys. Rev. Lett.*, 97(24):247401, 2006.
4. B. B. Buckley, G. D. Fuchs, L. C. Bassett, and D. D. Awschalom. Spin-light coherence for single-spin measurement and control in diamond. *Science*, 330(6008):1212–1215, 2010.
5. M. V. Gurudev Dutt, L. Childress, L. Jiang, E. Togan, J. Maze, F. Jelezko, A. S. Zibrov, P. R. Hemmer, and M. D. Lukin. Quantum Register Based on Individual Electronic and Nuclear Spin Qubits in Diamond. *Science*, 316(5829):1312–1316, 2007.
6. M. A. Nielsen and I. L. Chuang. *Quantum Computation and Quantum Information*. Cambridge University Press, Cambridge, 2000.
7. Jeremy L. O’Brien, Akira Furusawa, and Jelena Vuckovic. Photonic quantum technologies. *Nature Photon.*, 3(12):687–695, December 2009.
8. Igor Aharonovich, Andrew D. Greentree, and Steven Prawer. Diamond photonics. *Nature Photon.*, 5(7):397–405, July 2011.
9. Andrei Faraon, Paul E. Barclay, Charles Santori, Kai-Mei C. Fu, and Raymond G. Beausoleil. Resonant enhancement of the zero-phonon emission from a colour centre in a diamond cavity. *Nature Photon.*, 5(5):301–305, May 2011.
10. E. M. Purcell. Spontaneous emission probabilities at radio frequencies. *Phys. Rev.*, 69:681, 1946.
11. S. Tomljenovic-Hanic, MJ Steel, C.M. de Sterke, and J. Salzman. Diamond based photonic crystal microcavities. *Opt. Express*, 14(8):3556–3562, 2006.
12. I. Bayn and J. Salzman. Ultra high-Q photonic crystal nanocavity design: The effect of a low- ϵ slab material. *Opt. Express*, 16(7):4972–4980, 2008.
13. Andrei Faraon, Edo Waks, Dirk Englund, Ilya Fushman, and Jelena Vuckovic. Efficient photonic crystal cavity-waveguide couplers. *Applied Physics Letters*, 90(7):073102, 2007.
14. Andrei Faraon, Ilya Fushman, Dirk Englund, Nick Stoltz, Pierre Petroff, and Jelena Vuckovic. Dipole induced transparency in waveguide coupled photonic crystal cavities. *Opt. Express*, 16(16):12154–12162, Aug 2008.

15. B. P. Lanyon, J. D. Whitfield, G. G. Gillett, M. E. Goggin, M. P. Almeida, I. Kassal, J. D. Biamonte, M. Mohseni, B. J. Powell, M. Barbieri, A. Aspuru-Guzik, and A. G. White. Towards quantum chemistry on a quantum computer. *Nature Chem.*, 2(2):106–111, February 2010.